Tellus (1990), *42A*, 429–443

Normal mode projections of GCM response to tropical forcing

By WEILI ZHONG and JULIA NOGUES-PAEGLE, *Department of Meteorology, University of Utah, Salt Lake City, UT 84112, USA*

(Manuscript received 4 January 1989; in final form 18 July 1989)

ABSTRACT

The transient response of a general circulation model (GCM) is examined for the first 10 days of integration after a tropical heating source is switched on. Model output from 10 control and 10 experiment GCM runs are projected onto the normal modes of an adiabatic primitive equation model linearized about a basic state at rest to quantify the contributions from different modes to the 200 mb wind response. The response in the vicinity of the source is similar to that predicted by models linearized about uniform basic states, with important contributions from the internal Rossby and Kelvin modes in the tropics. The heating also excites internal gravity modes with contributions to the 200 mb winds about 40% of those of the internal Rossby modes through the 10-day integration time. The response in the external Rossby modes in the extratropics becomes statistically significant after 5 days. The internal mode contributions exhibit less spread from the ensemble average than those of external modes, a result due to the deterministic nature of the imposed heating.

1. Introduction

The structure of motions generated by tropical heating in a general circulation model (GCM) is described in terms of the projection of model output onto the three dimensional eigenfunctions of a linearized primitive equation model. The analysis is motivated by the lack of adequate knowledge of observed tropical forcing and its concomitant large scale atmospheric response.

Energy generated by release of latent heat by impulsively excited tropical convection radiates away in the form of inertia-gravity waves with only a small percentage remaining in the rotational circulation (Schubert et al., 1980). For atmospheric forcings with longer time scales, such as those that drive the Hadley cell, the resulting circulations contain non-negligible, inertia-gravity wave energy (Paegle, 1978; Puri, 1983; Paegle and Baker, 1983). This is particularly troublesome for the objective analyses used to produce gridded data which rely on assimilating models with a normal mode initialization step, which in their adiabatic formulations are known to suppress divergent motions (Bengtsson, 1981; Nogues-Paegle et al., 1986). Diabatic formulations have been proposed to remedy this problem (e.g., Wergen, 1983) which improve tropical divergent circulations and effectively control gravity wave noise resulting from data assimilation. Nevertheless, this solution is only accurate for modes whose natural frequency is much higher than that of the tropical forcing. Errico and Rasch (1988) have pointed out that this procedure fails when the forcing frequency approaches that of the natural frequency of the modes. This especially may occur for the eastward gravity modes which include the slowly moving Kelvin modes. Initialized fields will not accurately reproduce atmospheric levels of inertia-gravity wave energy in this case.

Forecasts for times longer than the model spin-up time may not suffer similar limitations if the model physics accurately reproduce tropical forcing. On the other hand, objective global analyses over data sparse regions will mostly reflect first guess values which are given by short range integrations of the assimilating GCM. This integration time, which is usually 6 h for operational forecasts, is not long enough to build up the tropical circulation which has been diminished by initialization. Therefore, quantification of the inertia-gravity wave response to tropical forcing in a GCM may be more instructive to learn about the atmospheric behavior of these modes, than similar studies based on analyzed fields.

This is the goal of the present study, which uses the numerical simulations done with the NCAR (National Center for Atmospheric Research) GCM by Paegle et al. (1987), hereafter referred to as PZB 87 to quantify the atmospheric response to tropical thermal forcing. The characteristics of the balance of different modes in this GCM has been investigated by Errico (1984). The present paper differs from his in that the characteristics of the response to a specified heating for a variety of initial conditions is investigated.

Section 2 describes the experiment and analyses techniques, Section 3 shows the characteristics of the averaged response while Section 4 contrasts tropical and extratropical response for different modes and ensemble members.

2. Experiment design

The numerical integrations were done with the 9 level NCAR GCM truncated at rhomoboidal 15 (R-15) as described in PZB 87. Williamson and Williamson (1984) and Ramanathan et al. (1983) have documented characteristics of the model which includes convective adjustment, solar and infrared radiation as well as surface drag and fluxes of temperature and moisture.

The integrations consist of ensembles of experiment and control cases started from 10 different dates of the 1979 winter selected by Baumhefner (1984). The integrations are carried out for 10 days and model output is saved in sigma coordinates for the initial 0.5, 1, 2, 3, 5, 7 and 10 day integration time. The experiment consists in adding a heating term to the thermodynamic energy equation in the region west of Central America centered at 6.6° N and 105° W decaying with a Guassian profile with half width of 15° in latitude and 30° in longitude, and a peak of 8 °C/day at 400 mb (PZB 87, Fig. 14). The ensemble average for day 10 shows a precipitation maximum over the heating region of 3.2 cm/day. The ensemble average response for the zonal wind at 200 mb exhibits maximum equatorial easterlies over the heating area, with westerlies to the east and extratropical westerlies in both hemispheres, colocated in longitude with the regions of maximum heating (PZB 87, Fig. 16). The discussion on this paper is limited to the given geometric design and location of the heating source. Simmons (1982) has shown that the tropical response is more sensitive to the vertical heating distribution than the extratropical response in linear models. He also discussed the dependance of the response on the latitude of the forcing.

Similar results were found by Nogues-Paegle and Mo (1988, hereafter referred to as NPM 88), in their study of the transient response of the southern hemisphere subtropical jet to tropical forcing. NPM 88 discussed the flow evolution in terms of eigenfunctions of a primitive equation model linearized about a basic state at rest, and found that changes in the subtropical jet are due to both changes in external and internal Rossby modes, while longitudinal changes in tropical heatings are reflected in similar shifts of the internal Kelvin and inertia-gravity modes. That paper did not investigate the partition of the response between Kelvin and Rossby modes in the tropics, which is of interest to the present investigation. Also, NPM 88 only carried out their integrations for one particular date, and therefore questions remain of whether similar results would be obtained for other initial conditions.

These points are addressed in the present paper by projecting the control and simulations performed by PZB 87 onto normal mode functions similar to those of NPM 88. These functions are obtained by separating the adiabatic primitive equations linearized about a basic state at rest into vertical and horizontal structure equations. The vertical structure equation is solved by finite difference approximations for the 9 model levels while the Hough functions, which are solutions of the horizontal structure equation are approximated as a series of associated Legendre polynomials (Kasahara and Puri, 1981). These correspond to those of the spectral GCM used here. The vertically varying basic state temperature is determined from the globally averaged temperature obtained from the ensemble average of the initial conditions. These basis functions are similar to those used in normal mode initialization and to those used by Kasahara (1984) to study the linear response of a stratified global atmosphere to thermal forcing.

Heights and winds at 9 sigma levels are then projected onto these functions separating the contributions from the first (external) vertical mode and vertical modes 2, 3, 4 and 5 (Fig. 1) and from each Hough function. Zonal and meridional winds are then reconstructed separately for Rossby, gravity, Kelvin and mixed Rossby-gravity modes. These are truncated to 12 zonal components and 10 and 6 meridional components for Rossby and gravity modes respectively. This truncation was chosen to reproduce most of the subtropical jet response produced by the R15 GCM. The 6 gravity mode components are the eastward and westward propagating gravity modes for the 3 largest meridional scales, which are expected to affect remote latitudes the most. The chosen truncation reproduces about 85% and 35% of the rotational and divergent wind response, respectively.

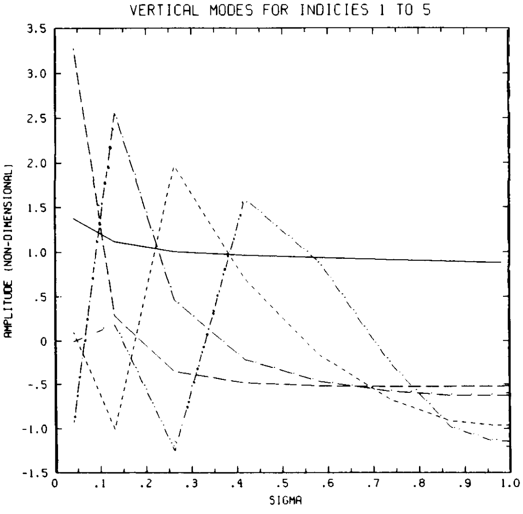

Fig. 1. The first 5 vertical structure functions for equivalent heights of 9556 m (—), 1979 m (--), 481 m (- o -), 164 m (---), and 65 m (-··-).

The reconstructed fields are projected back into sigma space separating the contribution from the external and the first four internal modes. Results are discussed in Section 3.

3. Normal mode projection of response

Contributions from the different modes and vertical structures for the u and v fields as described above are interpolated to 200 mb for depiction. At this level, the amplitude of the second vertical mode is negligible, and thus the internal mode variability shown here results mostly from vertical modes 3, 4 and 5. The significance of the response is quantified by the t statistics which normalize the difference of the ensemble averages between the controls and the experiments by the ensemble variability. These are computed as $t = (\overline{X}_1 - \overline{X}_2)\sqrt{18}/(S_1^2 + S_2^2)^{1/2}$ where $\overline{X}_1$ and $\overline{X}_2$ denote ensemble averages and S_1^2 and S_2^2 variances for the experiment and control respectively. They are shown in Figs. 2 through 6 for those projections for which the response has non-negligible amplitudes. The number of degrees of freedom for the ensemble differences between these 10 control and the 10 experiments is 18 for the case in which the variance of the two ensembles is the same. The similarity of the variance of the two ensembles was tested with an F-test (not shown) and found to be an acceptable statistical hypothesis over most of the grid points. Absolute values of t larger than 2.1 and 2.9 indicate that these ensemble averages are significantly different at the 95 and 99% level for these many degrees of freedom. This means that 1 out of 20 and 1 out 100 cases respectively, will have such values by chance with sample means actually coming from ensembles with the same average. By day 2, significant response is already felt by the contributions to the 200 mb zonal wind by the internal Rossby modes (Fig. 2), not only in the easterlies which develop over the heating region, and westerlies over the tropical Indian Ocean, but also in the subtropical jet to the south of the heating. On the other hand, significant differences in the external Rossby mode contributions (Fig. 3) are not felt until day 5 in the vicinity of the heating, and day 10 over the Indian Ocean.

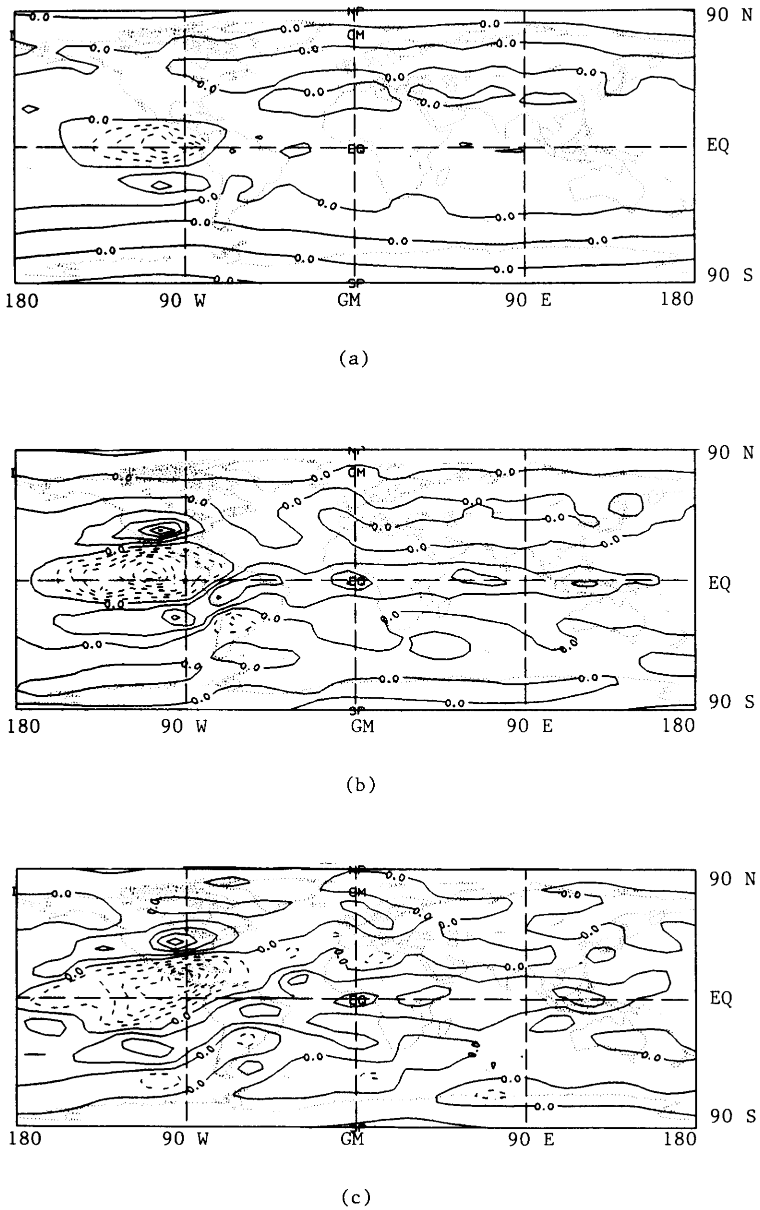

Fig. 2. T-statistics to test the statistical significance of the difference between the ensemble average for the experiment and the control for the contributions to the 200 mb zonal wind by the internal Rossby modes for integration times of 2 days (a), 5 days (b) and 10 days (c). The contour interval is 2.

Contributions by the internal gravity waves, both to the zonal (Fig. 4) and meridional (Fig. 5) components are immediately felt in the vicinity of the thermal source depicted by the t-statistics after 12 h of integration time. This is consistent with the linearized studies of Kasahara (1984) and Silva-Dias et al. (1983) which showed that forcings with short time scales tend to preferentially excite gravity waves. The subtropical jets' response are found poleward of the areas with

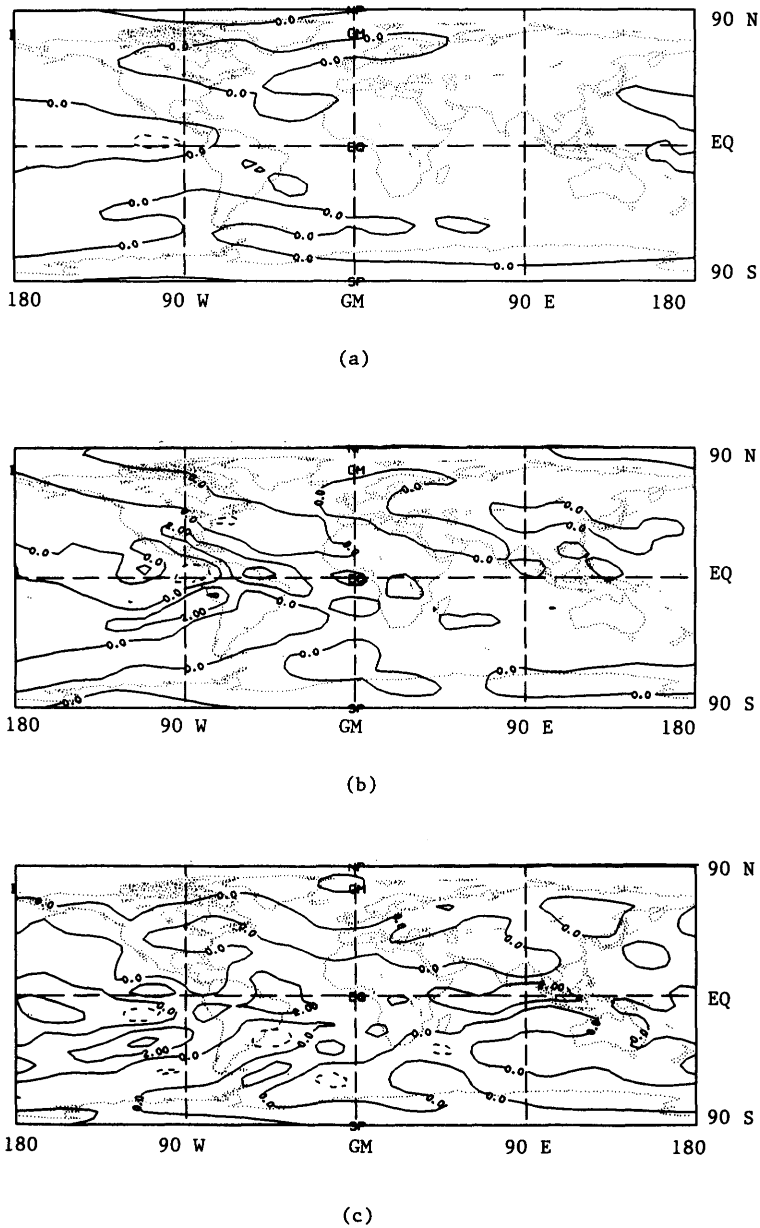

Fig. 3. Same as Fig. 2 but for contributions by external Rossby modes.

maximum contributions by inertial gravity waves to the meridional circulations, suggesting that at least partly, these accelerations are due to the forcing by the direct meridional overturnings generated by the thermal heating. Subsequent integration days also show gravity waves generated in the vicinity of large mountain ranges. These motions appear most clearly marked for the zonal wind component and result from the imbalances created close to the mountains by

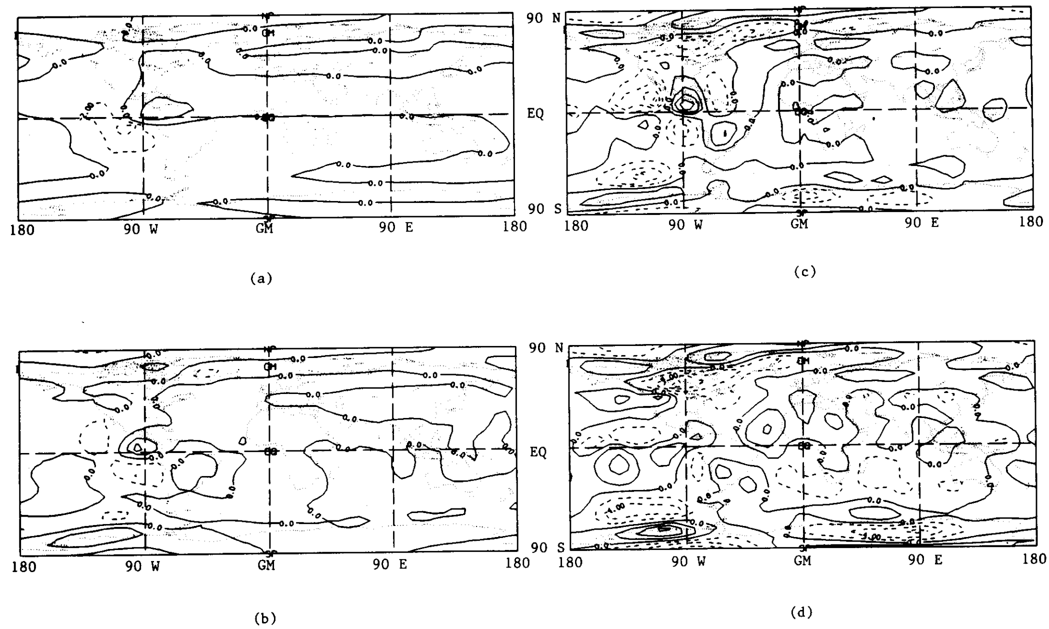

Fig. 4. Same as Fig. 2 but for contributions by internal gravity modes for integration times of 12 hours (a), 2 days (b), 5 days (c) and 10 days (d).

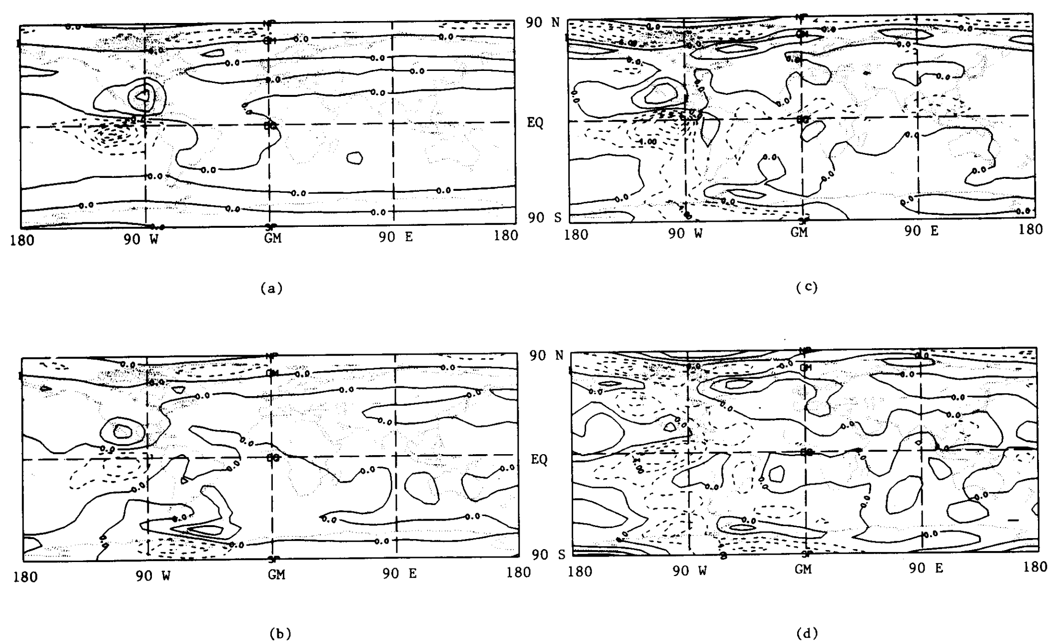

Fig. 5. Same as Fig. 4 but for contributions to the meridional wind at 200 mb by internal gravity waves.

motions induced by the heating. These tend to somewhat subside by day 10.

The t-statistics for the equatorially trapped modes (Fig. 6) exhibit significant response of the Kelvin mode, the easterly pulse propagating eastward with a speed of about 20 degrees of longitude per day. This is apparent in Fig. 6a, where the location of the leading westerly pulse is identified for four different integration times. The significant easterly pulse remains almost stationary west of the forcing. The mixed Rossby-gravity modes with zonal wavenumbers 6–7, are excited with significant response felt only after day 5.

The t-statistics are not useful for comparison of the relative strength of the ensemble response for the different modes because of the normalization by the standard deviation of the ensembles. Thus, Figs. 7 and 8 depict the actual (i.e., non-normalized) 200 mb zonal wind response for days 5 and 10, respectively. At day 5, the contributions to the zonal wind in the vicinity of the source from the external Rossby, internal Kelvin and other gravity waves included here have maximum values of similar magnitudes. On the other hand, the internal Rossby modes contribute twice as much as the other modes. A preferential response in baroclinic structures due to a parabolic forcing in the vertical was also found in the linear studies of Lim and Chang (1983) and Kasahara (1984).

By day 10, the meridional propagation of an external Rossby wave front is apparent in the western half of the Southern Hemisphere, with peak values in the subtropics there of similar magnitudes for the internal and external modes.

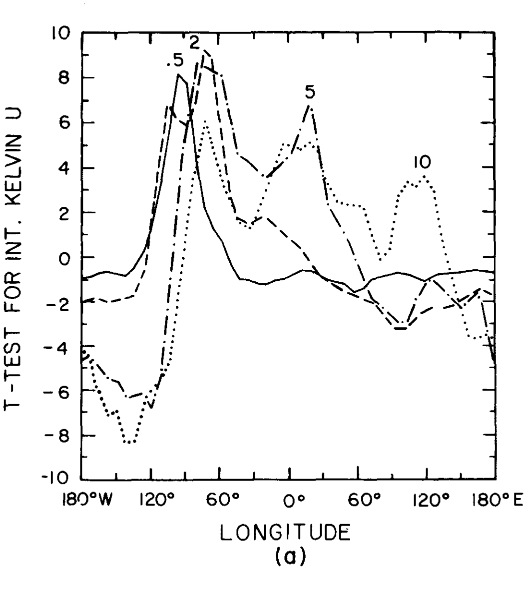

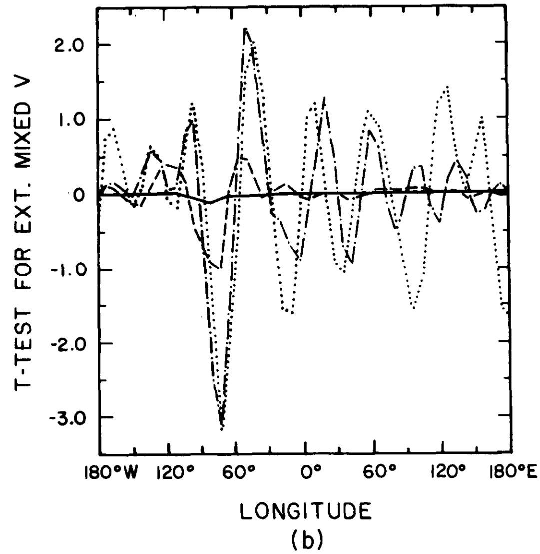

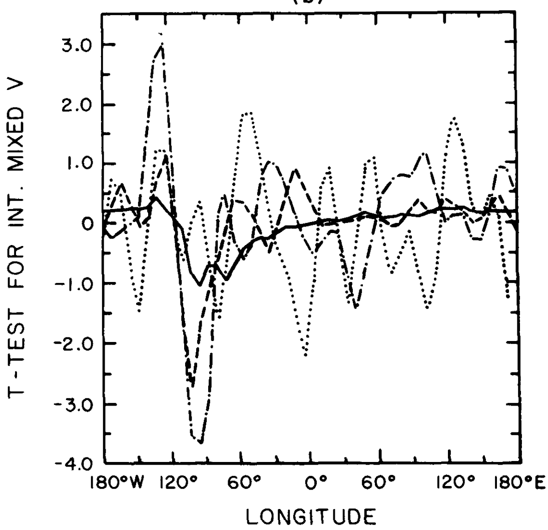

Fig. 6. Equatorial values of the t-test for contributions of Kelvin modes to the 200 mb zonal wind (a), and of external (b), and internal (c) mixed gravity-Rossby modes to the 200 mb meridional wind. Solid line shows value at 0.5 day, dash line at 2 days, dash-dot line at 5 days and dot line at 10 days.

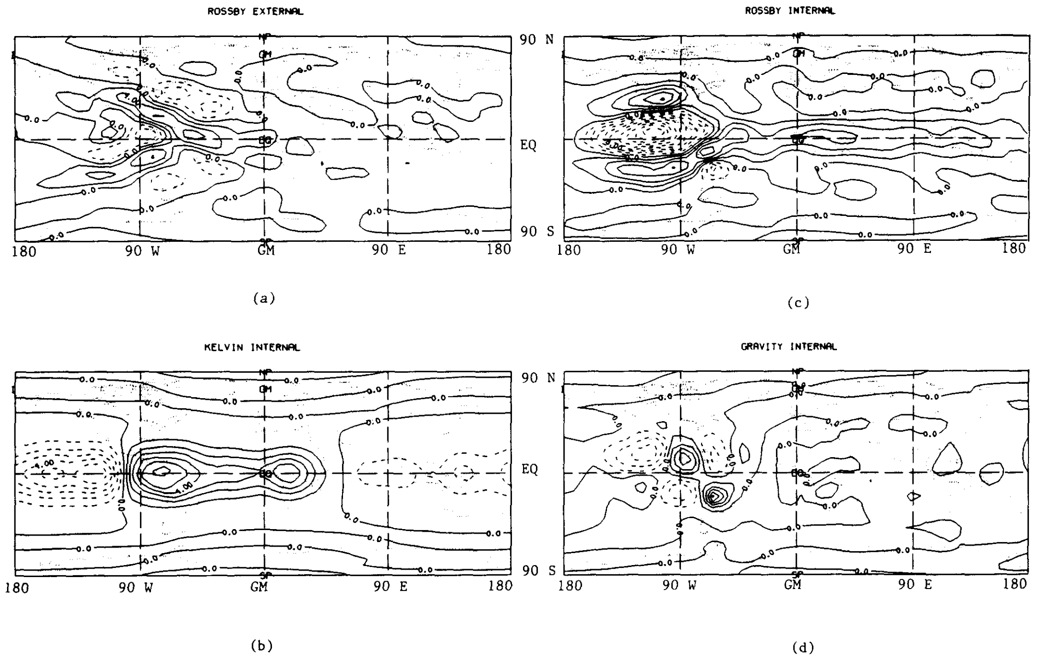

Fig. 7. Contribution to the 200 mb zonal wind response by external (a) and internal (c) Rossby modes, internal Kelvin (b) and internal gravity (d) modes for integration day 5. Contour interval of (a) and (c) is 2 m/s and for (b) and (d) is 1 m/s. Negative values are dashed.

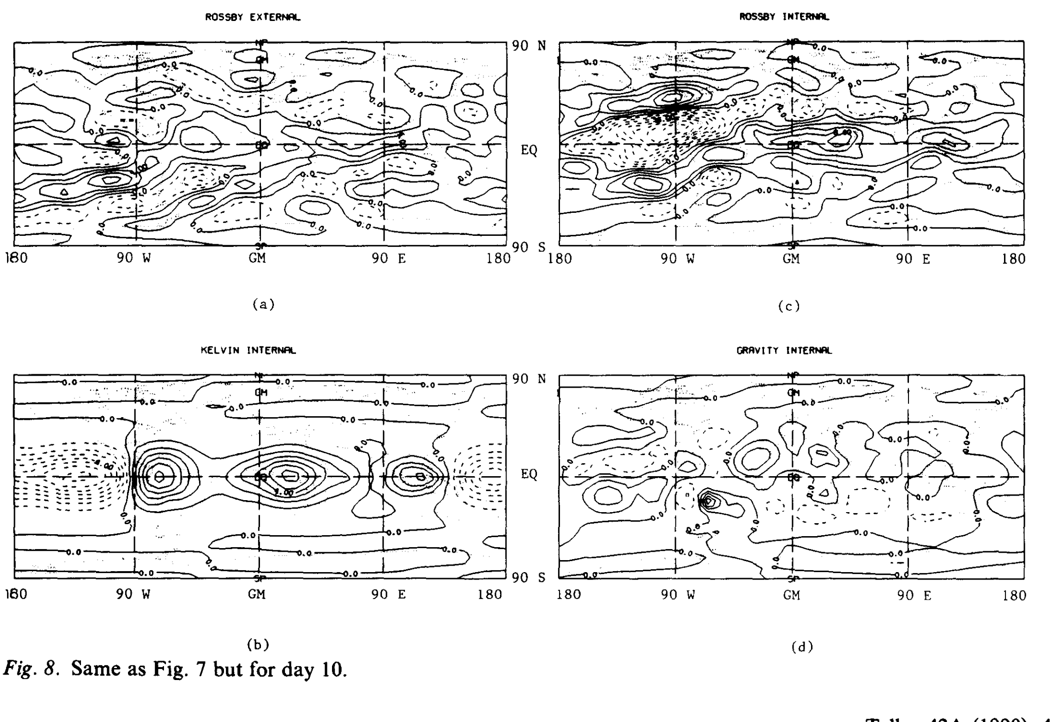

Fig. 8. Same as Fig. 7 but for day 10.

The excitation of a barotropic response in the extratropics from parabolic heating in linear models has been related to the vertical shear of the actual zonal wind (e.g., Simmons, 1982; Kasahara and Silva-Dias, 1986). The response of the present non-linear calculations have many features similar to those obtained in linear models, particularly the Kelvin and Rossby mode response close to the source during the first 5 days of integration and the excitation of extratropical barotropic modes at later times.

On the other hand, the Rossby mode contribution to the elongated westerlies east of the forcing is larger than that of the Kelvin mode. This is different than what is predicted for the stationary response of a linearized model by Gill (1980) which shows the westerlies to the east of the forcing to be due mostly to the Kelvin mode. The easterlies over the heating result mostly from internal Rossby modes, partly compensated by Kelvin mode westerlies, a feature common to both the GCM and linear solutions.

This section has emphasized the mean response, which smooths random differences caused by the different initial conditions of the ensemble members. Section 4 will show that some of the response features discussed here are still apparent when individual ensemble members are considered.

4. Ensemble member behavior

In this section the wind vector response R_c is separately calculated for tropical and middle latitudes as follows:

$$R_c = \left(\frac{1}{A} \int_A R_c^2 \, da \right)^{1/2} \quad \text{with} \quad R_c^2 = |V_{\text{exp}}^{\text{C}} - V_{\text{control}}^{\text{C}}|^2,$$

and with the area A defined to extend from 25° N to 25° S, (tropics) and from 25° N to 75° N and from 25° S and 75° S (mid latitudes). The ensemble mean is also computed as:

$$R = \left(\frac{1}{10} \sum_{c=1}^{10} R_c^2 \right)^{1/2}$$

averaging over the 10 cases. The resulting values are plotted in Fig. 9 comparing the tropical against the extratropical response for each ensemble member. By day 10, the response in the external Rossby mode for mid-latitudes is comparable in magnitude to that of the internal Rossby modes in the tropics. The averaged amplitude of this measure for the internal gravity waves (excluding the Kelvin and mixed Rossby-gravity modes) in the tropics is about 40% of that of the internal Rossby modes. The internal gravity wave response is better trapped in the tropics for all ensemble members than that of the internal Rossby modes.

This last characteristic is more obvious for latitudinal averages computed as:

$$R(\phi) = \left(\frac{1}{10} \sum_{c=1}^{10} \frac{1}{2\pi} \int_0^{2\pi} |V_{\text{exp}}^{\text{C}} - V_{\text{control}}^{\text{C}}|^2 \, d\lambda \right)^{1/2},$$

where ϕ is the latitude and λ is the longitude. This is plotted versus latitude for the original data before projection, and for different mode projections in Figs. 10 and 11. Fig. 10a shows the response to be confined mostly to tropical latitudes during the first 5 days integration time, while the extratropical response becomes apparent after 5 days. The extratropical response at day 10 is about 50% stronger than the internal Rossby response in the Northern (winter) Hemisphere while it is closer to the internal Rossby response in the Southern (summer) Hemisphere (Fig. 10b and c). The zonally averaged Rossby mode response appears to propagate meridionally at a speed of about 20° latitude per week, though the phase speed of propagation of the Rossby wave front response is faster than this. The internal gravity modes remain more confined to tropical latitudes than do the Rossby modes, with peak values found about 20° north and south of the heating maximum. These peak values are about half the magnitude of the internal Rossby modes at similar latitudes. In the deep tropics the existence of an oscillatory behavior in the gravity waves, with an apparent period of 5 days is evident. Errico (1984) determined for the CFM an important diabatic forcing with this frequency for the internal gravity modes. The current experiment may be exciting a similar frequency that causes this period to be apparent in the response. At the equator itself, the largest contributions are due to the Kelvin and mixed gravity-Rossby modes, with peak values at day 10 about half the value of the internal Rossby modes there. The mixed mode also exhibits non-negligible amplitudes in

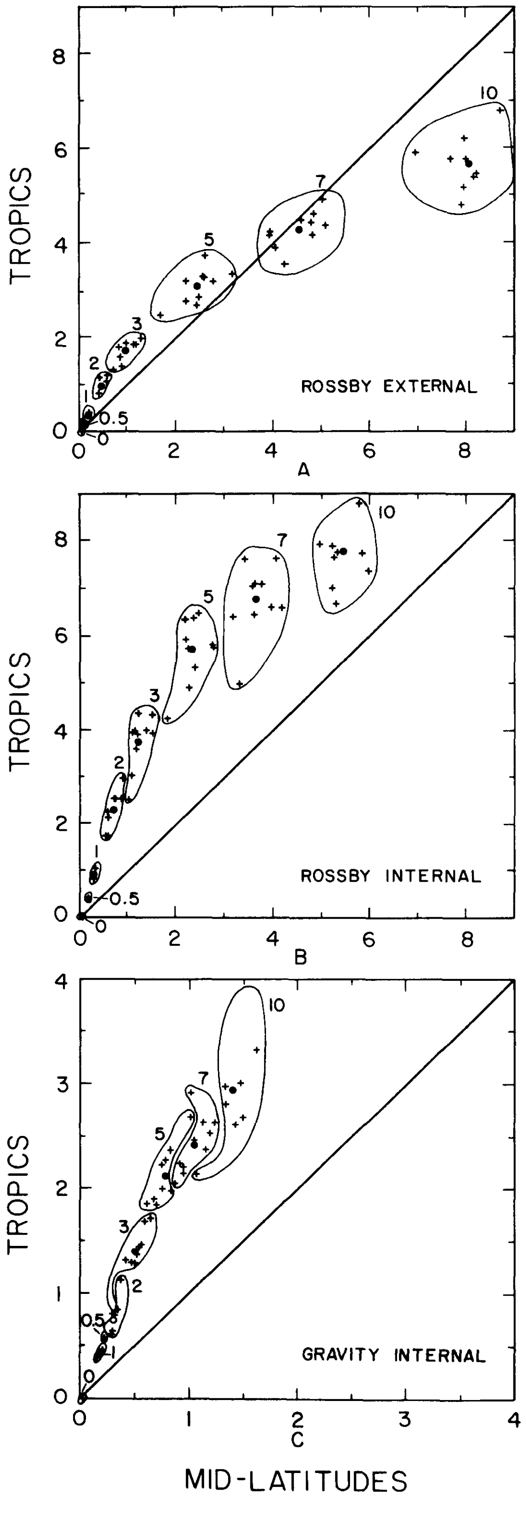

the external component, which due to its larger meridional scale, impacts also in subtropical latitudes.

We have so far discussed only the nature of the response through two particular measures: the average response and the wind vector response. It is also of interest to quantify the contributions to the ensemble variance σ^2 by each ensemble member σ_c^2 and to compare this with the magnitude of the average wind response AR where

$$\mathrm{AR} = \left(\frac{1}{A}\int_A |\bar{V}_{\exp} - \bar{V}_{\mathrm{control}}|^2 \, \mathrm{d}a\right)^{1/2}$$

with $\bar{V} = \frac{1}{10}\sum_{c=1}^{10} V^c$.

This comparison gives an idea of the magnitude of the spread from the ensemble averaged response due to different initial conditions. This is given in Fig. 12 where:

$$\sigma_c = \left(\frac{1}{A}\int_A |V^C_{\exp} - V^C_{\mathrm{control}} - (\bar{V}_{\exp} - \bar{V}_{\mathrm{control}})|^2 \, \mathrm{d}a\right)^{1/2}$$

and the ensemble standard deviation is given by

$$\sigma = \left[\frac{1}{10}\sum_{c=1}^{10} \sigma_c^2\right]^{1/2}.$$

The ensemble variance for the tropics and extratropics is given by the average of the squares of each point in the ensemble clouds. Its square root (ensemble standard deviation) is given by the heavy dot. Comparison of the standard deviation to the average wind response shows that by day 10 of the integration, the ratio between the ensemble standard deviation of the extratropical Rossby response and that of the ensemble wind response is about 3.5, while these ratios are about 2.5 and 2 for the gravity and internal Rossby modes respectively. This is to be expected since the internal modes are responding more directly to the forcing, while the extratropical response in

Fig. 9. Wind response R_c for each ensemble member (+) and their ensemble mean R (•) for the tropics and mid-latitudes, for 0.5, 1, 2, 3, 5, 7 and 10 day integration time. Curves enclose ensemble members at given times. Units are m/s. Values above/below the diagonal indicate preferred response in the tropics/mid-latitudes. Contributions from Rossby external modes are shown in (a), from Rossby internal modes in (b) and from gravity internal modes in (c).

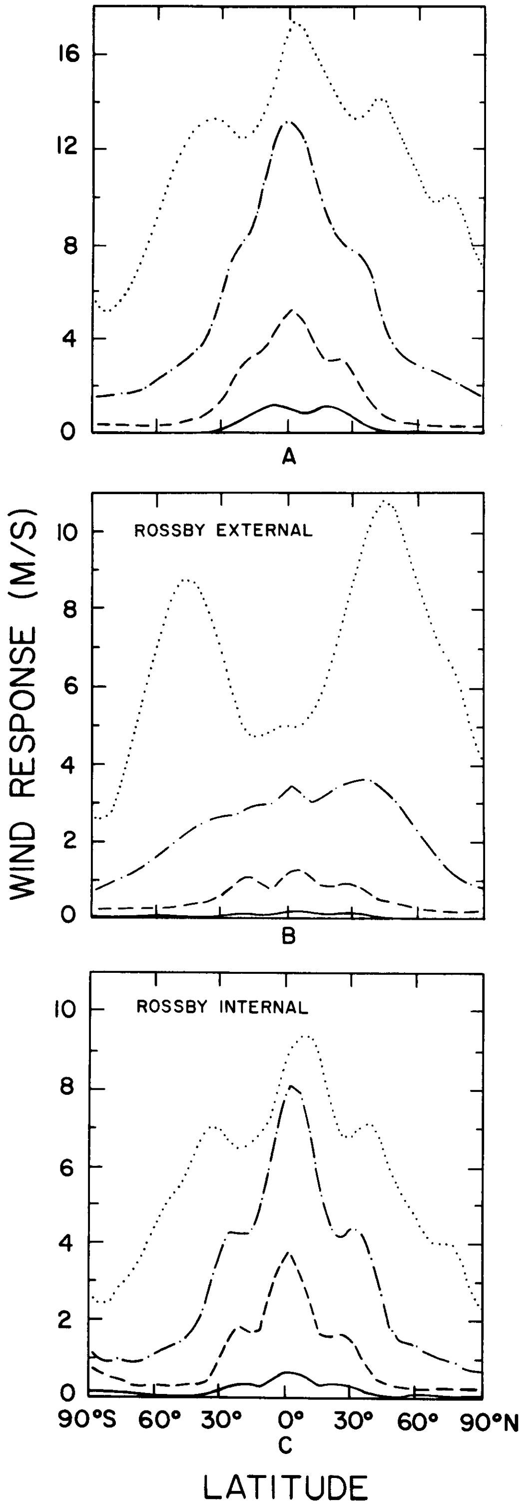

the external mode results from the propagation of these modes through a spatially variable basic state (e.g., Branstator, 1983) or through non-linear effects, which add random signals from the different ensemble members.

5. Summary and conclusions

GCM integrations of an experiment designed to study the non-linear response of the atmosphere to tropical heating have been analyzed to quantify the strength of the response of structures which project onto the linear modes of a primitive equation model linearized about a basic state at rest. These functions are similar to those used in normal mode initialization of general numerical models, which is obtained through a short range integration of the assimilating GCM. This integration time still reflects the initialized conditions in regions with low observation densities, which may be missing important contributions to the internal gravity modes even in the case of diabatic initialization (Errico and Rasch, 1988).

Our discussion focusses on the 200 mb wind rather than height field, since wind variations are of similar magnitudes in the tropics as in mid-latitudes, unlike height fields which display negligible tropical gradients. The normal mode analyses imply particular relationships between the height and wind fields, and therefore the three dimensional fields of heights as well as winds are needed for the present study. The GCM response close to the heating bears similarities to predictions from models linearized about uniform basic states, but it is quite different for remote regions. We find that strong tropical heating quickly generates significant response in both internal gravity and Rossby waves. The ratio of the wind response between these two quantities remains at about 40% throughout the 10 day integration time. Extra-tropical response is apparent in the external

Fig. 10. Latitudinal distribution of wind response $R(\phi)$ (m/s). Total values are shown in (a), contributions from external and internal Rossby modes are shown in (b) and (c) respectively. Solid line shows value at 0.5, dash line at 2, dash-dot line at 5 and dot line at 10 days respectively.

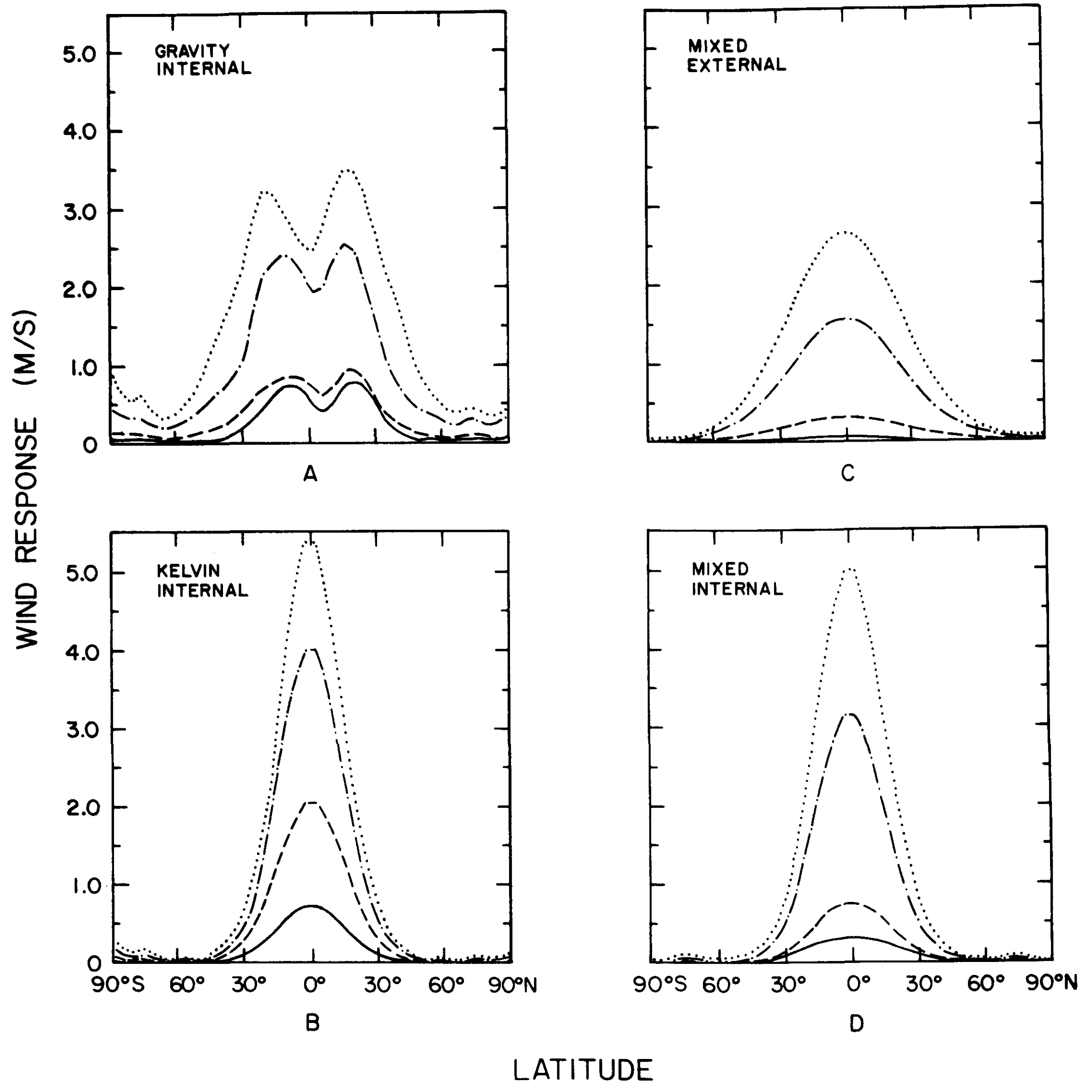

Fig. 11. Same as Fig. 10 but for contributions from gravity internal (a), Kelvin internal (b), and mixed gravity-Rossby modes external (c) and internal (d).

Rossby modes by day 5. From this time on, these modes contribute 50 to 75% to the response of the 200 mb wind poleward of 40° latitudes. It is of interest that some of the features described here for the atmospheric response to tropical heating are similar to those found by Nogues-Paegle et al. (1986) in their analyses of observed global fields. It was found there that weekly averages of

Fig. 12. Average wind response AR for the tropics and mid-latitudes for contributions from Rossby external (a), Rossby internal (c) and gravity internal modes (e). σ_c (+) and σ (•), for the tropics and mid-latitudes, for contributions from Rossby external (b), Rossby internal (d) and gravity internal modes (f). Units are m/s. Numbers in figures indicate integration time (days). Values above and below diagonal indicate largest variability in tropics and mid-latitudes respectively.

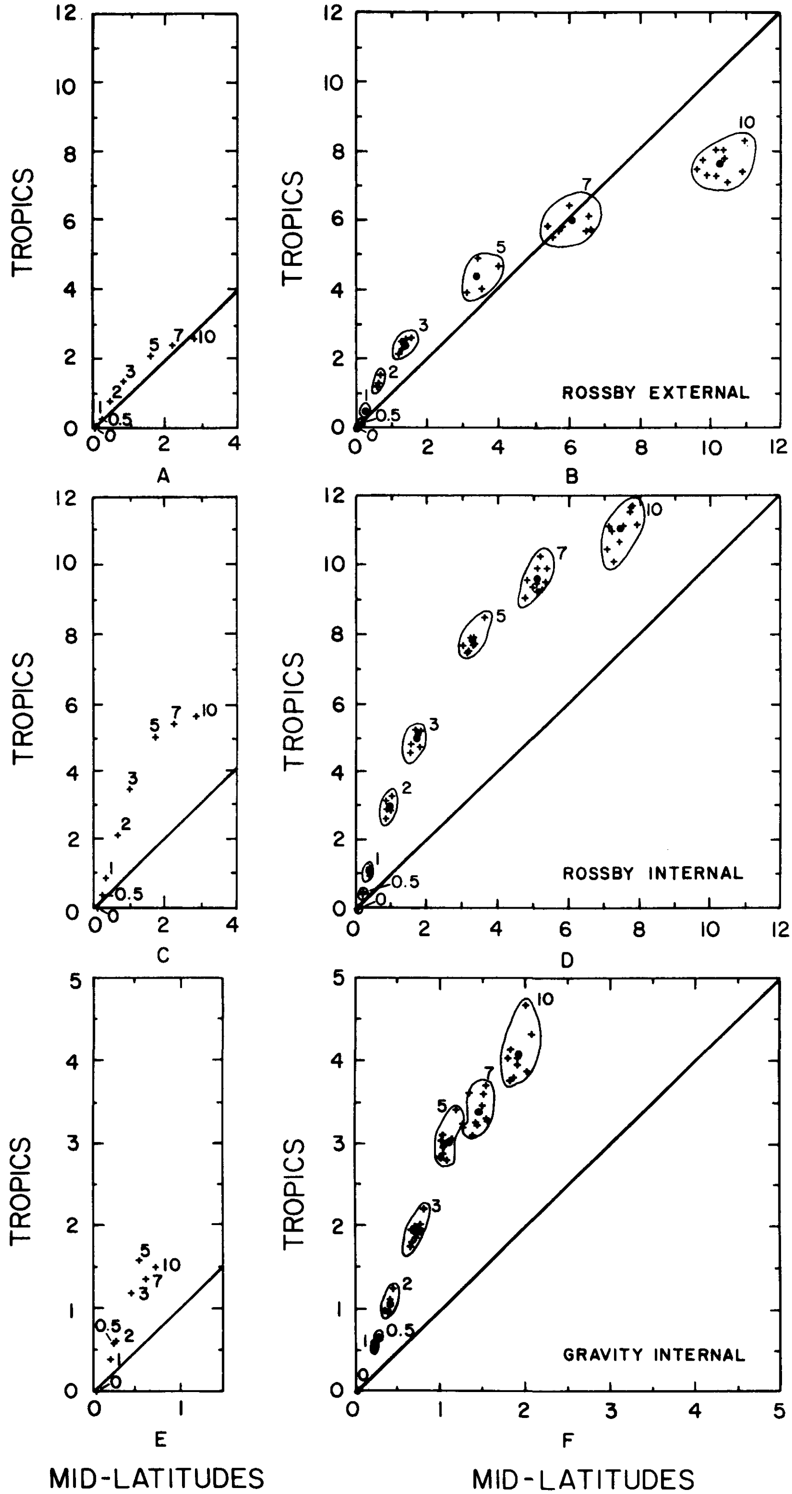

TROPICS
MID-LATITUDES
A
B
C
D
E
F
ROSSBY EXTERNAL
ROSSBY INTERNAL
GRAVITY INTERNAL

large-scale flow exhibit a predominant internal structure. The results presented here justify our previous conjecture that such structures are due to tropical heating.

That study also showed contributions from the internal gravity modes of about 50% of those of the internal Rossby modes. Comparisons among different analyses systems reported in that study showed the sensitivity of this result to the analyses system. It was then concluded that the high levels of gravity wave energy may have been an artifact of the analyses systems. Our current conclusions, though, support this level of internal gravity wave energy between 30° N and 30° S in the vicinity of strongly heated regions. More accurate observations of tropical forcings and related circulations are needed before a definite conclusions can be reached about the reality of this level of gravity wave energy on observed atmospheric motions.

The 10-day integrations discussed here also permits us to draw some conclusions about the time scales in which tropical forcing may be expected to influence higher latitudes. This may be of utility to determine the scale at which systematic tropical errors will influence higher latitudes. Significant response in the internal Rossby modes is already apparent at 2 days, while those of the internal gravity modes are already apparent at 12 h. By day 5, the response of the external Rossby modes becomes of similar magnitude as that of the internal modes in the subtropics. By day 10, significant response is found in the extratropics, and is dominated by the external Rossby mode.

6. Acknowledgements

This work has been jointly supported by NSF grants ATM 8613347 and 8611952 and NASA grant NAG 5-127. We are grateful to R. Errico for his interest and helpful comments.

REFERENCES

Baumhefner, D. P. 1984. Analysis and forecast intercomparisons using the FGGE SOP-I data base. *FGGE Workshop*, Woods Hole, Mass., National Academy of Sciences, 228–246. (Available from USC-GARP, National Academy of Sciences, 2101 Constitution Ave., Washington, D.C., 20418).

Bengtsson, L. 1981. Current problems in four-dimensional data assimilation. *Data Assimilation Methods, ECMWF Seminar* 1980, 195–217. (Available from the European Centre for Medium Range Weather Forecasts, Shinfield Park, Reading RG2 9AX, England).

Branstator, G. 1983. Horizontal energy propagation in a barotropic atmosphere with meridional and zonal structure. *J. Atmos. Sci. 40*, 1689–1708.

Errico, R. M. 1984. The dynamical balance of a general circulation model. *Mon. Wea. Rev. 112*, 2439–2454.

Errico, R. M. and Rasch, P. J. 1988. A comparison of various normal-mode initialization schemes and the inclusion of diabatic processes. *Tellus 40A*, 1–25.

Gill, A. E. 1980. Some simple solutions for heat-induced tropical circulation. *Quart. J. Roy. Met. Soc. 106*, 447–462.

Kasahara, A. and Puri, K. 1981. Spectral representation of three-dimensional global data by expansion in normal mode functions. *Mon. Wea. Rev. 109*, 37–51.

Kasahara, A. 1984. The linear response of a stratified global atmosphere to tropical thermal forcing. *J. Atmos. Sci. 41*, 2217–2237.

Kasahara, A. and Silva Dias, P. L. 1986. Response of planetary waves to stationary tropical heating in a global atmosphere with meridional and vertical shear. *J. Atmos. Sci. 43*, 1893–1911.

Lim, H. and Chang, C. P. 1983. Dynamics of teleconnections and Walker circulations forced by equatorial heating. *J. Atmos. Sci. 40*, 1897–1915.

Nogues-Paegle, J., Zhen, Z., Sampson, G. and Paegle, J. 1986. Vertical structure of the wind field during the Special Observing Period I of the global weather experiment. *Meteor. Atmos. Phys. 35*, 149–165.

Nogues-Paegle, J. and Mo, K. C. 1988. Transient response of the Southern Hemisphere subtropical jet to tropical forcing. *J. Atmos. Sci. 45*, 1493-1508.

Paegle, J. 1978. The transient mass-flow adjustment of heated atmospheric circulations. *J. Atmos. Sci. 35*, 1678–1688.

Paegle, J., Zhang, C.-D. and Baumhefner, D. P. 1987. Atmospheric response to tropical thermal forcing in real data integrations. *Mon. Wea. Rev. 115*, 2975–2995.

Paegle, J. and Baker, W. E. 1983. The influence of the tropics on the prediction of ultralong waves. Part II: Latent heating. *Mon. Wea. Rev. 111*, 1350–1371.

Puri, K. 1983. The relationship between convective adjustment, Hadley circulation, and normal modes of the ANMRC spectral model. *Mon. Wea. Rev. 111*, 23–33.

Ramanathan, V., Pitcher, E. J., Malone, R. C. and Blackmon, M. L. 1983. The response of a spectral general circulation model to refinements in radiative processes. *J. Atmos. Sci. 40*, 605–630.

Schubert, W. H., Hack, J. J., Silva-Dias, P. L. and Fulton, S. R. 1980. Geostrophic adjustment in an axisymmetric vortex. *J. Atmos. Sci. 37*, 1464–1484.

Silva-Dias, P. L., Schubert, W. H. and DeMaria, M. 1983. Large scale response of the tropical atmosphere to transient convection. *J. Atmos. Sci. 40*, 2689–2707.

Simmons, A. J. 1982. The forcing of stationary wave motions by tropical diabatic heating. *Quart. J. Roy. Meteor. Soc. 108*, 503–534.

Wergen, W. 1983. Initialization. *Interpretation of Numerical Weather Prediction Products*, ECMWF Seminar/Workshop 1982. 31–57. (Available from the European Centre for Medium Range Weather Forecasts, Shinfield Park, Reading RG2 9AX, UK).

Williamson, D. L. and Williamson, G. S. 1984. Circulation statistics from January and July simulation with the NCAR climate Model (CCMOB). *NCAR Technical Note TN-244+STR*, 112 pp. (Available from the National Center for Atmospheric Research, P.O. Box 3000, Boulder, Colorado 80307, USA).